BioMed Central

Research article

Heterotrimeric G protein subunits are located on rat liver endosomes

Rebecca W Van Dyke*

Address: Dept of Internal Medicine, University of Michigan School of Medicine and Veterans Administration Hospital, Ann Arbor, MI 48105, USA

Email: Rebecca W Van Dyke* - wynne@umich.edu

* Corresponding author

Abstract

Background: Rat liver endosomes contain activated insulin receptors and downstream signal transduction molecules. We undertook these studies to determine whether endosomes also contain heterotrimeric G proteins that may be involved in signal transduction from G protein-coupled receptors.

Results: By Western blotting $G_{s\alpha}$, $G_{i\alpha1,2}$, $G_{i\alpha3}$ and G_β were enriched in both canalicular (CM) and basolateral (BLM) membranes but also readily detectable on three types of purified rat liver endosomes in the order recycling receptor compartment (RRC) > compartment for uncoupling of receptor and ligand (CURL) > multivesicular bodies (MVB) >> purified secondary lysosomes. Western blotting with antibodies to Na, K-ATPase and to other proteins associated with plasma membranes and intracellular organelles indicated this was not due to contamination of endosome preparations by CM or BLM. Adenylate cyclase (AC) was also identified on purified CM, BLM, RRC, CURL and MVB. Percoll gradient fractionation of liver postnuclear supernatants demonstrated co-occurrence of endosomes and heterotrimeric G protein subunits in fractions with little plasma membrane markers. By confocal microscopy, punctate staining for $G_{s\alpha}$, $G_{i\alpha3}$ and G_β corresponded to punctate areas of endocytosed Texas red-dextran in hepatocytes from control and cholera toxin-treated livers.

Conclusion: We conclude that heterotrimeric G protein subunits as well as AC likely traffic into hepatocytes on endosome membranes, possibly generating downstream signals spatially separate from signalling generated at the plasma membrane, analogous to the role(s) of internalized insulin receptors.

Background

Heterotrimeric G proteins, important for signal transduction in hepatocytes, attach through lipid modifications to the cytoplasmic face of plasma membranes, particularly lipid rafts, where they interact with G protein coupled-receptors (GPCR) to initiate signal transduction [1,2]. $G_{s\alpha}$, $G_{i\alpha1,2}$, $G_{i\alpha3}$ and G_β have been identified on rat liver basolateral (BLM) and canalicular (CM) membranes [3,4].

Although current concepts of signal transduction envision interaction of the cytoplasmic tails of activated receptors with intracellular signal transduction cascades at the plasma membrane, insulin and epidermal growth factor (EGF) receptors and some GPCRs are internalized in endocytic vesicles [2,5-8]. GPCRs such as the β_2 adrenergic receptor are endocytosed with β-arrestins which regulate receptor desensitization and recycling [2].

Further, the internalized receptors with β-arrestins contribute to the assembly of internalized signalling complexes and MAPK activation [2]. In rat liver activated insulin and EGF receptors continue to generate signals from endosomes [5,7] and critical elements of mitogen-activated protein kinase (MAPK) signalling pathways are found on endosomes [6,9]. Little is known, however, regarding whether heterotrimeric G proteins involved in cAMP signalling pathways and effectors like adenylate cyclase (AC) are located on endocytic vesicles. The observations that in vitro GTP-γS stimulates acidification of rat liver endosomes [10], that liver endosomes exhibit protein kinase A (PKA) activity [10] and that both $G_{i\alpha3}$ and regulators of G protein signalling are located on rat liver "carrier" vesicles where they may alter endosome function [11] suggest that heterotrimeric G proteins may be localized to endosomes, play a role in vesicle trafficking and possibly transduce signals from the cytosol, spatially separated from plasma membranes. Further, in renal cells, $G_{i\alpha}$ and PKA are found on endosomes [12,13] and antibodies to $G_{s\alpha}$, $G_{i\alpha2}$ and $G_{i\alpha3}$ label cytoplasmic vesicles near apical and basolateral membranes [14] while $G_{s\alpha}$ and $G_{i\alpha3}$ are found on Golgi membranes in renal and pancreatic cells [14,15]. Complex interactions may exist between heterotrimeric G proteins and endosomes as heterotrimeric G proteins or cAMP may alter fusion and/or trafficking of intracellular vesicles [16], including endosomes [17] and Golgi secretory vesicles [14]. Finally some GPCRs, notably the β_2-adrenergic receptor, are regulated by endo- and exocytosis [2].

This study was undertaken to determine whether heterotrimeric G protein subunits are localized to liver endocytic vesicles or lysosomes. Well characterized preparations of rat liver secondary lysosomes and three types of endocytic vesicles were employed, including: 1) compartment for uncoupling of receptor and ligand (CURL), "sorting endosomes" that mediate separation of endocytosed receptors and their ligands [18-22]; 2) recycling receptor compartment (RRC), vesicles recycling receptors back to the plasma membrane from CURL with some transcytotic vesicles and early endosomes [22,23]; and 3) multivesicular bodies (MVB), late endosomes that contain endocytosed ligands transferred from CURL, en route to lysosomes for degradation [18,19,22-24].

Results
Western blotting
By Western blotting, $G_{s\alpha}$, $G_{i\alpha1,2}$, $G_{i\alpha3}$ and G_β were detected on all samples of CM and BLM in amounts greater than in homogenate (2.3–3.4-fold, $p \leq 0.0006$ except for $G_{i\alpha1,2}$ in BLM;1.6-fold, $p = 0.079$) (Figure 1) with slightly more in CM than BLM ($p = $ NS except for $G_{i\alpha1,2}$, $p = 0.022$). $G_{s\alpha}$, $G_{i\alpha1,2}$, $G_{i\alpha3}$ and G_β were detected in most samples of vesicles (n = 7–9): RRC (100%), CURL (75–100%), MVB

(63–100%) and lysosomes (50–100%) (Figure 1, data not shown) although quantitatively at lower levels than CM and BLM ($p < 0.0001$ to $p = 0.027$) or homogenate ($p < 0.0001$ to p=NS), indicating the bulk of these proteins was on plasma membranes. $G_{s\alpha}$, $G_{i\alpha1,2}$, and G_β were detected on vesicles in the order RRC>CURL>MVB, lysosomes. For $G_{i\alpha3}$ the order was RRC>CURL, MVB>lysosomes (p values are indicated in Figure 1). The order RRC>CURL>MVB is that identified for recycling receptors for asialoglycoproteins, low density lipoproteins and EGF [18,19,23,24].

Although RRC, CURL, MVB and lysosomes are considered clean [18-25], contamination by CM or BLM containing large amounts of G proteins is an important issue. Therefore BLM, CM, endosomes and lysosomes were examined for the quantity and/or relative distribution of marker proteins. The plasma membrane marker Na, K-ATPase exhibits variable ratios of α/β subunits: intracellular membranes>>>apical>basolateral membranes [3,26,27], attributed to differential trafficking [26] and turnover [28]. Both subunits were identified on CM and BLM, however BLM exhibited more β_1 than CM (Figure 2). α_1 was detected in vesicles in the order RRC>CURL>MVB>lysosomes (RRC vs. MVB, $p = 0.012$; RRC vs. lysosomes, $p = 0.001$; CURL vs. lysosomes, $p = 0.004$) (Figure 2). However β_1 was not detected in intracellular vesicles (Figure 2). The antibodies were capable of detecting both subunits in BLM over a wide range of protein (2.5–60 μg), including amounts of BLM (2.5–5 μg) in which α_1 optical density was similar to that of 60 μg of RRC and CURL (Figure 2B). Therefore, the α/β ratio in vesicles does not support contamination by plasma membranes.

Other membrane-associated marker proteins were examined qualitatively (Figure 3). Rab 5a and rab 4 bind to early and recycling endosomes, respectively [29] and were detected on CM and BLM but not on vesicles. Transferrin receptor (Trf-R) recycles between BLM and TGN/recycling vesicles [17,19,23,30,31] and was detected on BLM>CM and vesicles in the order RRC>CURL>MVB. Two CM proteins that undergo endocytosis, MDR-related protein 2 (MRP-2) and multi-drug resistance protein 1 (MDR-1) [32-34], exhibited a different order: MVB>CURL>RRC>lysosomes. Collectively these findings suggest that simple contamination of intracellular vesicles by CM or BLM cannot account for the presence of heterotrimeric G protein subunits in vesicles as otherwise G proteins and these other proteins should have been found on vesicles in the same order.

Percoll gradient fractionation
To further address issues of localization and contamination and to avoid bias due to selective loss of some organelles, liver PNS was fractionated on Percoll
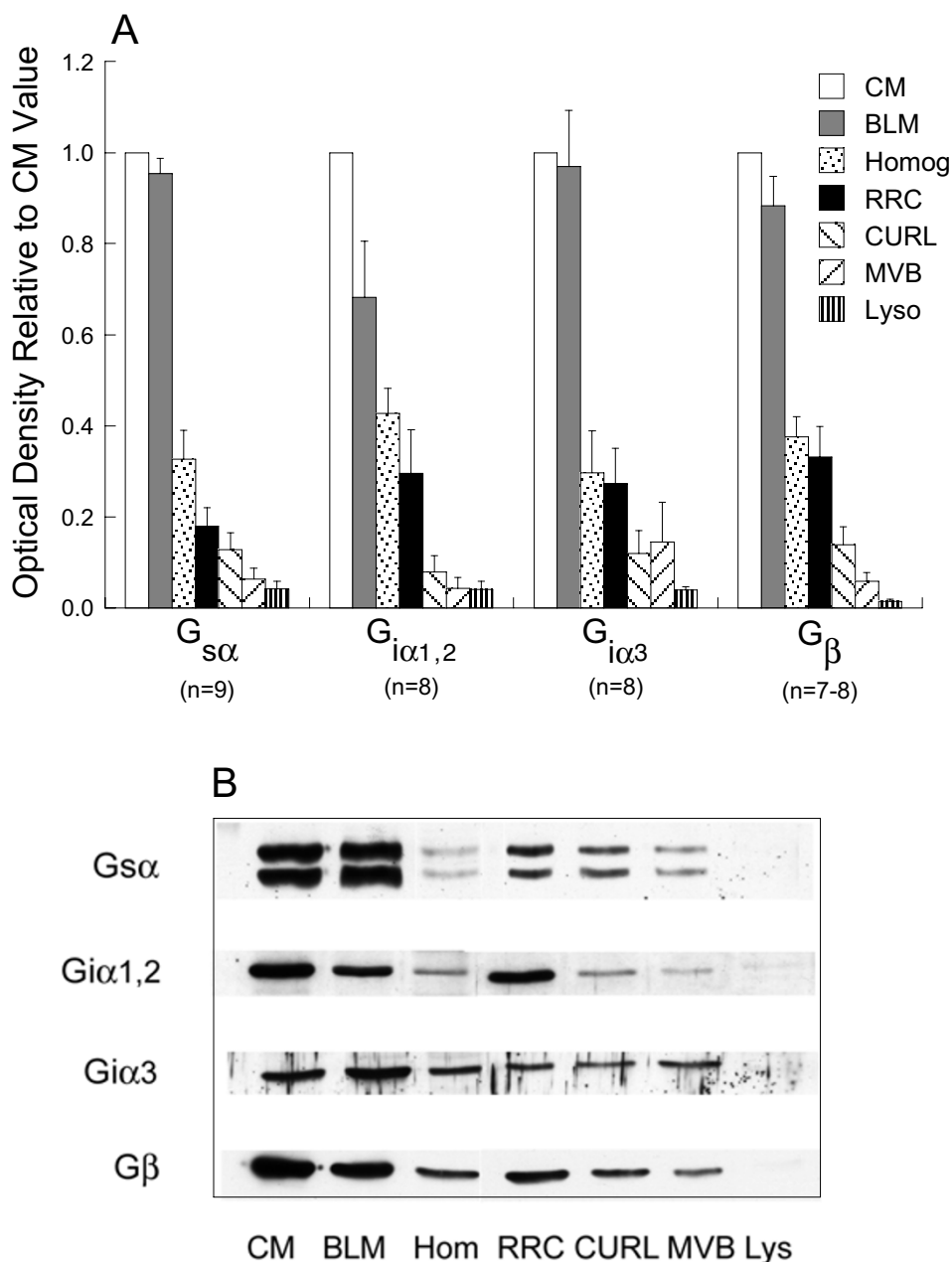
Figure 1
G proteins on endosomes and membranes. A) Quantitative distribution of $G_{s\alpha}$, $G_{i\alpha1,2}$, $G_{i\alpha3}$ and G_β in different cell fractions: CM (white bars), BLM (gray bars), liver homogenate (dotted bars), RRC (black bars), CURL (down slashed bars), MVB (up slashed bars) and lysosomes (stripped bars). Optical density of bands for each cell fraction on a single blot were expressed as a fraction of the optical density of the band for CM on the same blot and bars represent the mean ± SEM of results from "n" different preparations of each cell fraction, as indicated on the figure. Except for $G_{i\alpha1,2}$ in BLM, G protein subunits were enriched significantly in CM and BLM compared to homogenate ($p < 0.0006$). G protein subunits in endosomes and lysosomes were significantly less than in CM or BLM ($p < 0.0001$ to $p = 0.027$). In vesicles $G_{s\alpha}$, $G_{i\alpha1,2}$, and G_β were found in the order RRC > CURL > MVB > lysosomes and $G_{i\alpha3}$ in the order RRC > CURL, MVB > lysosomes. Many of these differences achieved statistical significance: $G_{s\alpha}$: RRC vs MVB, $p = 0.027$; RRC vs lysosomes, $p = 0.007$; CURL vs lysosomes, $p = 0.049$. $G_{i\alpha1,2}$: RRC vs CURL, $p = 0.05$; RRC vs lysosomes, $p = 0.022$. $G_{i\alpha3}$: RRC vs lysosomes, $p = 0.01$. G_β: RRC vs CURL, $p = 0.032$; RRC vs MVB, $p = 0.002$; RRC vs lysosomes, $p = 0.0006$; CURL vs lysosomes, $p = 0.008$. B) Representative Western blots illustrating data summarized in (A). $G_{s\alpha}$: 15 μg protein/lane; others: 30 μg protein/lane; Hom: homogenate.
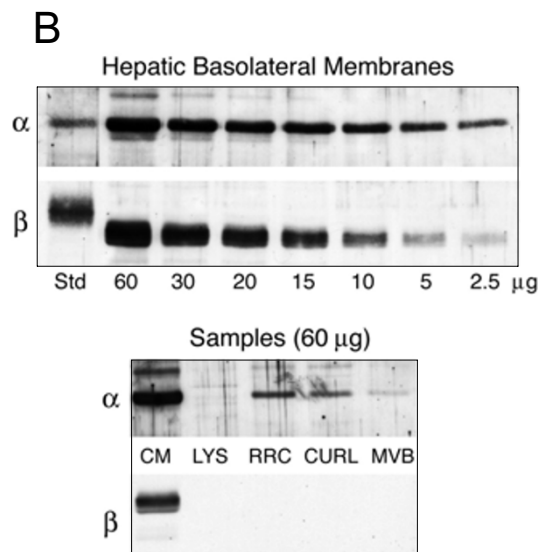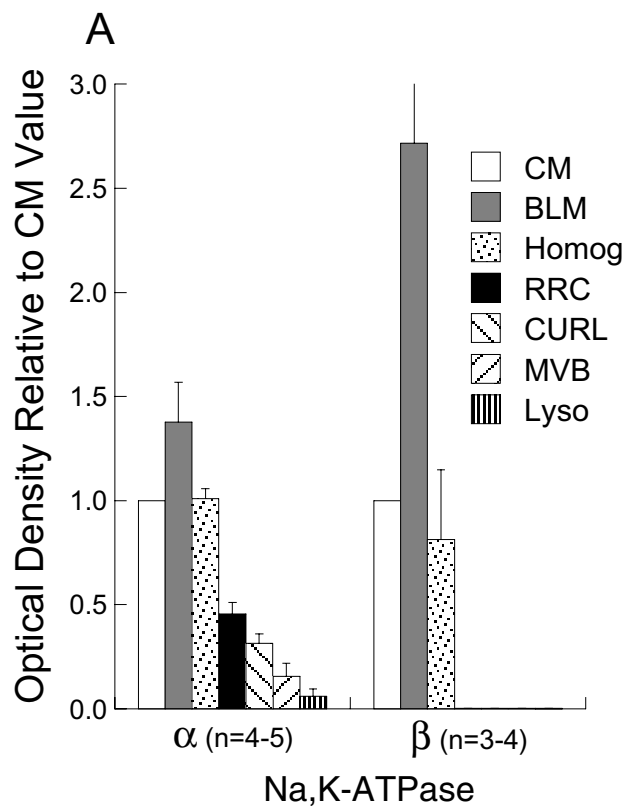
Figure 2
Na, K-ATPase as membrane marker. A) Quantitative distribution of $\alpha 1$ and $\beta 1$ subunits of Na, K-ATPase in different cell fractions: CM (white bars), BLM (gray bars), liver homogenate (dotted bars), RRC (black bars), CURL (down slashed bars), MVB (up slashed bars) and lysosomes (stripped bars). Optical densities were normalized to values in CM as in Figure 1. Bars represent the mean ± SEM of results from "n" different preparations of each cell fraction, as indicated on the figure. Both subunits were disenriched in endocytic vesicles and lysosomes compared to CM ($p < 0.0001$). B) Upper blot: detection of $\alpha 1$ and $\beta 1$ subunits in BLM over a wide range (2.5–60 μg) of protein/lane. Lower blot: representative Western blot illustrating data summarized in (A) with 60 μg protein/lane.
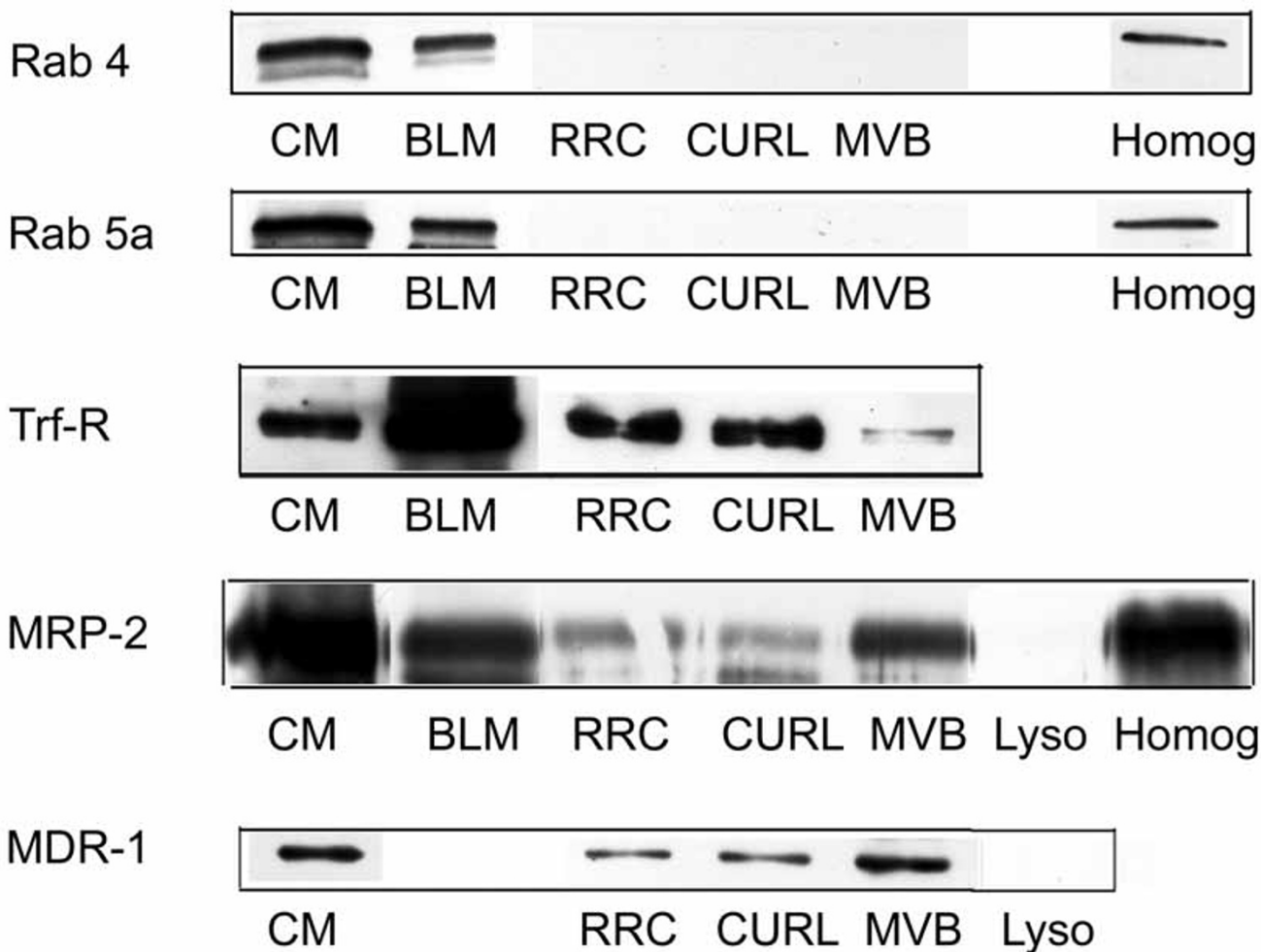
Figure 3
Plasma membrane proteins on endosomes. Detection of various plasma membrane-associated proteins in purified endocytic vesicles and lysosomes. For rab 4, rab 5a and transferrin receptor (Trf-R) lanes contained 100 μg, 100 μg and 30 μg protein, respectively and blots shown are representative of studies of 6–10, 6–10 or 2 different preparations of each cell fraction, respectively. For MRP-2 and MDR-1, lanes contained 100 μg of protein except for CM (10 μg and 5 μg, respectively) and BLM (10 μg) and blots shown are representative of studies of 4–12 and 17–19, respectively, different preparations of each cell fraction.

gradients. Fractions were examined for the pattern of distribution of the entire population of liver endosomes and lysosomes (identified from internalized fluorescein isothiocyanate-dextran (FITC-dextran) as described [17]), heterotrimeric G protein subunits and marker proteins (Figure 4). APDE I and FITC-wheat germ agglutinin (WGA) were assessed to identify plasma membranes [15,17]. (The data for FITC-dextran and APDE I were published as part of another figure [17]). Low density fractions 29–30 contain cytosol while fractions 20–28 contain most plasma membranes and endosomes.

Although plasma membrane markers were detected throughout the gradient, relatively little was measured in fractions 5–15, compared to fractions 20–28. However, endosomes were distributed throughout the gradient, including dense lysosomes (fractions 3–6) with lysosome-associated membrane protein 1 (LAMP1). Indeed in fractions 6–14, FITC-dextran-containing endosomes were found at mean levels up to 35% of levels in the peak endosome fractions 23–27. Similarly, rab 5a, which binds early endosomes and early endosome antigen 1 (EEA1) [29], was readily detectable throughout the gradient. EEA1,
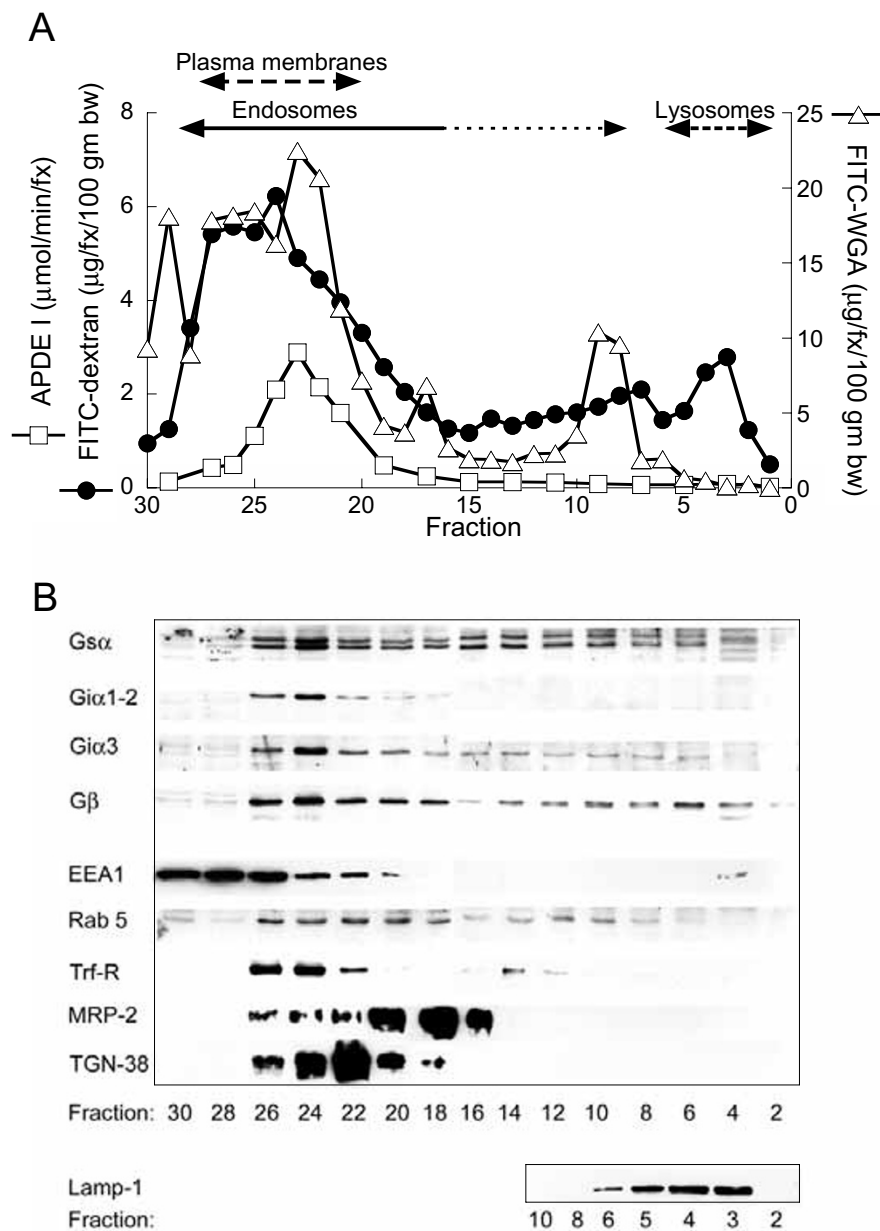
Figure 4
Distribution of G proteins on Percoll gradients. A) Distribution of endocytosed FITC-dextran (closed circles), BLM-bound FITC-WGA (open triangles) and the plasma membrane marker alkaline phosphodiesterase 1 (APDE 1) (open squares) on Percoll gradients. The predominant positions of plasma membranes, endosomes and lysosomes are indicated at the top of the graph. The data for the dextran and APDE 1 curves were previously published [ref [17], Figure 3C]. Reprinted from Hepatology 32, Van Dyke RW, Effect of cholera toxin and cyclic adenosine monophosphate on fluid phase endocytosis, distribution and trafficking of endosomes in rat liver, pp. 1357–1369, 2000 with permission from The American Association for the Study of Liver Disease. B) Distribution of $G_{s\alpha}$, $G_{i\alpha1,2}$, $G_{i\alpha3}$ and G_β and various marker proteins on Percoll gradients. Blots for heterotrimeric G protein subunits contained 20 μg protein/lane and are representative of similar blots for 4 different liver preparations. Blots for EEA1, rab 5, Trf-R, MRP-2, TGN-38 and LAMP1 contained 40, 20, 20, 30, 30 and 15 μg protein/lane, respectively, and are representative of similar blots for 4,4,4,4,3 and 4 different liver preparations, respectively.
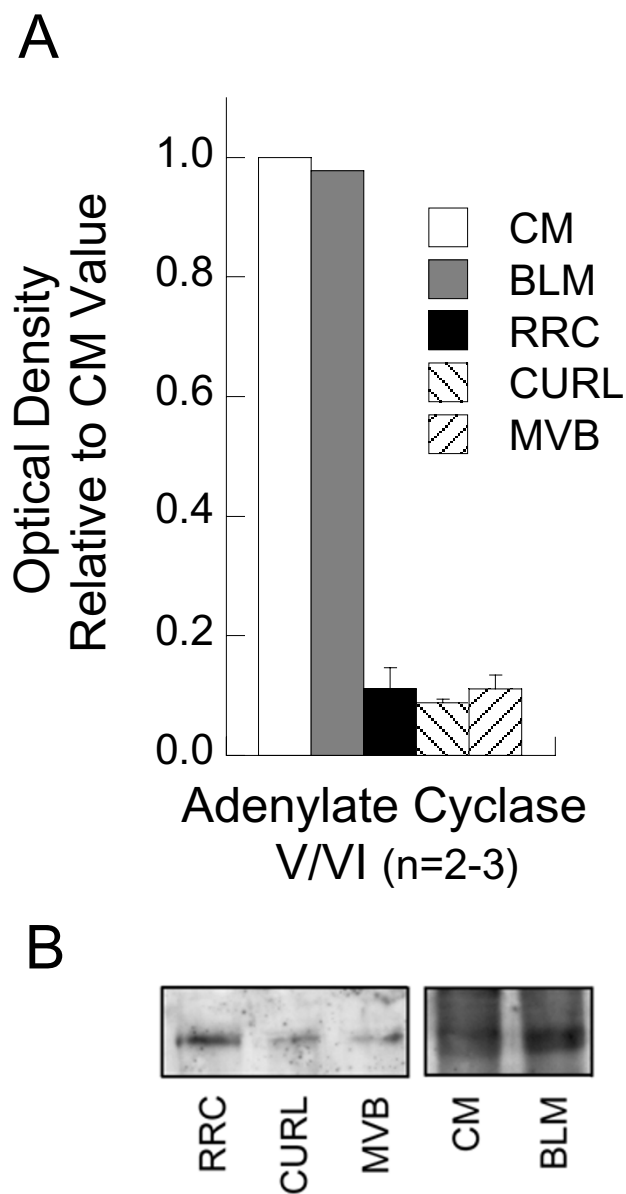
A

B

Figure 5
Adenylate cyclase on endosomes. A) Quantitative distribution of AC in different cell fractions: CM (white bars), BLM (gray bars), RRC (black bars), CURL (down slashed bars) and MVB (up slashed bars). Optical densities were normalized to values for CM as in Figure 1. Bars represent mean ± SEM of results from 2 different preparations of BLM and 3 preparations each of RRC, CURL and MVB. RRC, CURL and MVB exhibited significantly less AC compared to CM (p ≤ 0.0003). B) Representative Western blots showing detection of AC in CM and BLM (30 μg protein/lane) and in purified endocytic vesicles (60 μg protein/lane).

however, was detected primarily only in cytoplasm (fractions 29–30) and overlapping plasma membranes/endosomes in fractions 22–28. Trans-Golgi network protein 38 (TGN-38) localized to fractions 18–26, marking primarily the TGN [17]. Trf-R localized primarily to fractions 22–26, likely indicating plasma membranes, recycling endosomes and the TGN/Golgi [17,30]. MRP-2 localized to fractions 16–26, overlapping plasma membranes and endosomes.

$G_{s\alpha}$, $G_{i\alpha3}$ and G_{β} were identified readily throughout the gradient, principally in membrane/endosome fractions 18–26, but also in denser fractions 4–18, a pattern similar to rab 5a and FITC-dextran (Figure 4). The similar distribution of endocytosed FITC-dextran, $G_{s\alpha}$, $G_{i\alpha3}$ and G_{β} and rab 5a, in a pattern distinct from that of other marker proteins, suggests that $G_{s\alpha}$, $G_{i\alpha3}$ and G_{β} are located on intracellular vesicles. $G_{i\alpha1,2}$ exhibited a different pattern, limited to fractions 18–26, overlapping most endosomes/plasma membranes.

Adenylate cyclase localization
AC, a major effector for $G_{s\alpha}$, also was detected on CM, BLM and, in smaller amounts (p ≤ 0.0003), on RRC, CURL and MVB (Figure 5). The antibody employed detects both AC V/VI. AC VI is expressed in liver, regulated positively by $G_{s\alpha}$ and negatively by $G_{i\alpha}$ [35] and likely is the protein identified in the present studies.

Confocal microscopy
Confocal microscopy was employed to look for colocalization of $G_{s\alpha}$, $G_{i\alpha1,2}$, $G_{i\alpha3}$ and G_{β} with internalized Texas red-dextran, a marker of fluid phase endocytosis from the BLM [17]. As previously described [17], endocytosed dextran is found in characteristic locations. Texas red-dextran, endocytosed for 2 minutes, identified punctate structures (early endosomes) beneath BLM in untreated (Figures 6A,7A,7E,8A) or cholera toxin (CTX)-treated (Figure 8C) animals. Faint punctate structures (arrows, Figure 6A,7E,8A) in the pericanalicular area represent autofluorescent lipofuscin [17]. After 20 minutes of endocytosis (Figures 6C,7C,7G,8E), dextran was observed in punctate structures near CM (arrows), representing "later" endosomes and lysosomes [17]. In CTX-treated livers Texas red-dextran was visible also in punctate perinuclear structures (arrows, Figure 6E; arrowheads, Figure 8G) that represent mistrafficked early and late endosomes [17].

In control livers (Figures 6B,6D) antibody to $G_{s\alpha}$ heavily stained BLM and CM and lightly stained nuclei and small punctate structures near both membranes. Arrows point to overlap of Texas red-dextran fluorescence and $G_{s\alpha}$ staining (Figures 6C,6D). This pattern of linear membrane and punctate vesicular labelling has been previously described for other membrane proteins subject to endo-and
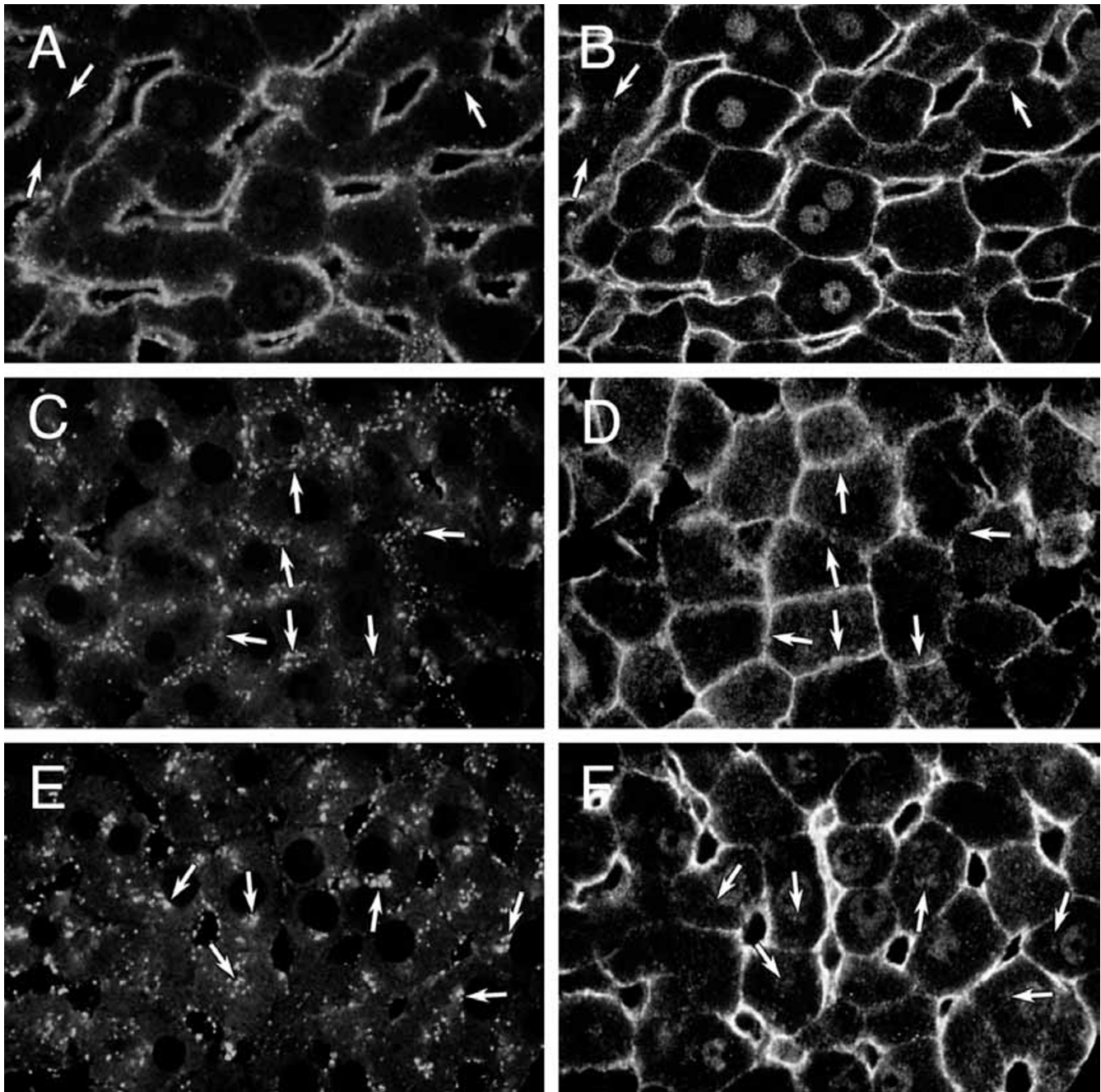
Figure 6
G$_{s\alpha}$ on endosomes. Confocal microscopy of rat liver sections showing distribution of endocytosed Texas red-dextran (A, C, E) and G$_{s\alpha}$ (B, D, F) in the same, respective, images. A, B: Control liver exposed to dextran for 2 minutes. Arrows point to punctate G$_{s\alpha}$ staining in the pericanalicular area (B) and region where faint punctate autofluorescence was visible(A). C, D: Control liver exposed to dextran for 20 minutes. Arrows point to punctate G$_{s\alpha}$ staining in the pericanalicular area (D) and corresponding endocytosed Texas red-dextran (C). E, F: CTX-treated liver exposed to dextran for 20 minutes. Arrows point to punctate G$_{s\alpha}$ staining in the perinuclear area (F) and corresponding endocytosed Texas red-dextran (E). All images were obtained with anti-fluorescein Alexa 488 amplification of signal and are representative of 16 (A, B), 54 (C, D) and 56 (E, F) images examined from 1, 6 and 6 livers, respectively.
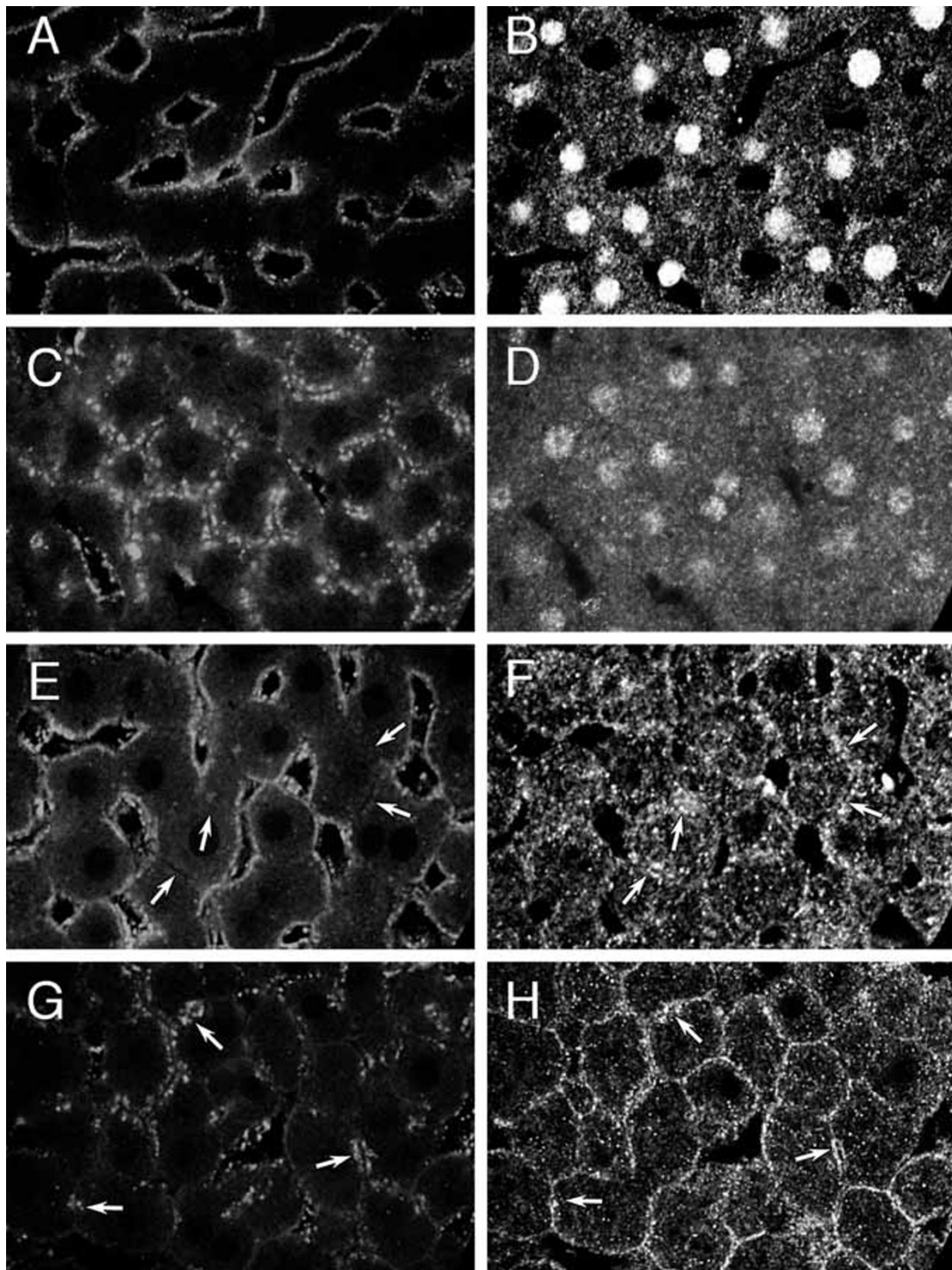
Figure 7
$G_{i\alpha1,2}$ and $G_{i\alpha3}$ on endosomes. Confocal microscopy of rat liver sections showing distribution of endocytosed Texas red-dextran (A, C, E, G) and $G_{i\alpha1,2}$ (B, D) or $G_{i\alpha3}$ (F, H). $G_{i\alpha1,2}$: A, B: Control liver exposed to dextran for 2 minutes. C, D: Control liver exposed to dextran for 20 minutes. $G_{i\alpha3}$: E, F: Control liver exposed to dextran for 2 minutes. G, H: Control liver exposed to dextran for 20 minutes. Arrows point to punctate $G_{i\alpha3}$ staining in the pericanalicular area (F, H) and region of punctate autofluorescence (E) or corresponding endocytosed Texas red-dextran (G). Images D and H were obtained with anti-fluorescein Alexa 488 amplification of signal. Images A-H are representative of 17 (A, B), 52 (C, D), 11 (E, F) and 50 (G, H) images examined from 1, 7, 1 and 7 different livers, respectively.
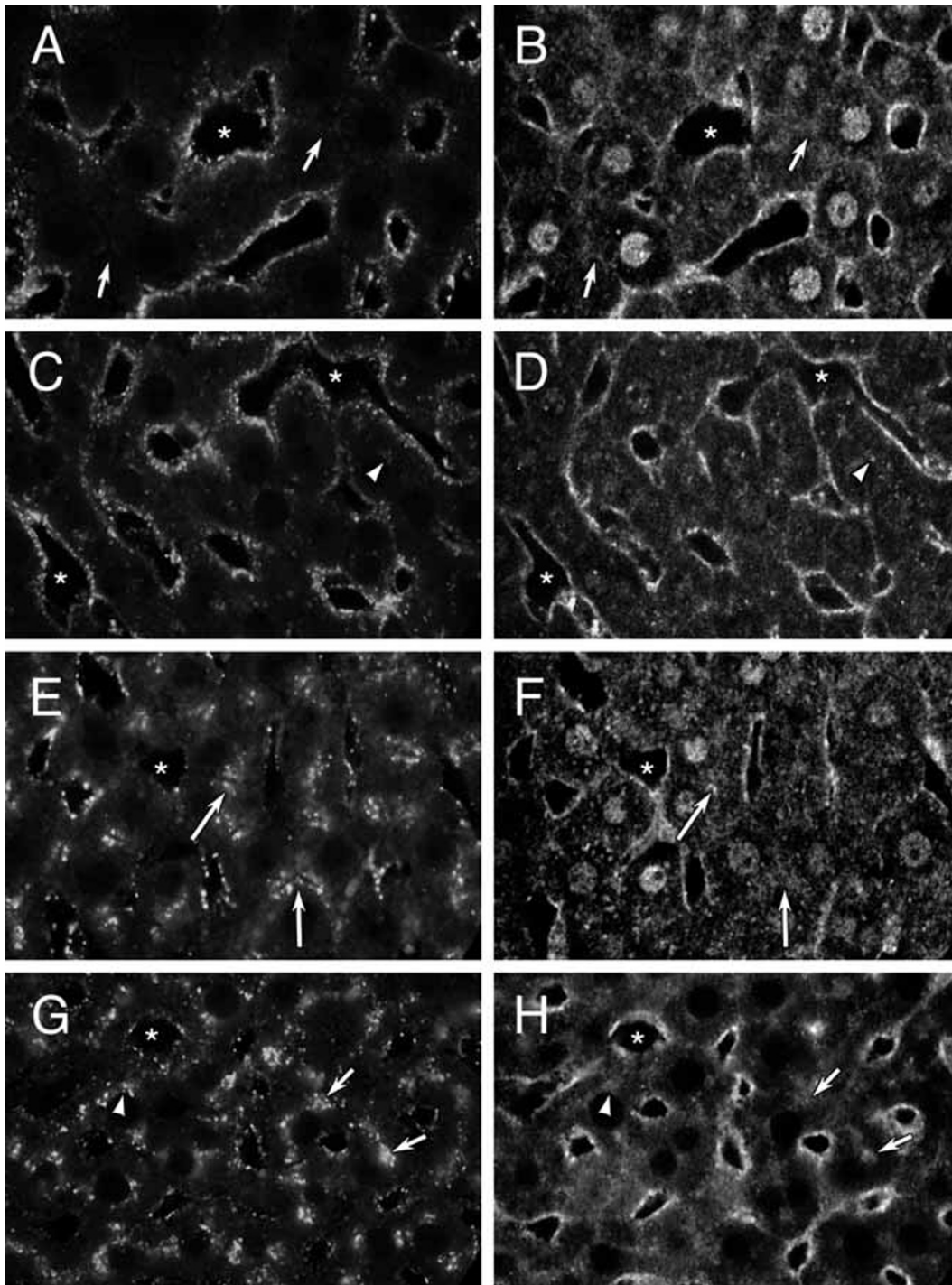
Figure 8
G_β **on endosomes.** Confocal microscopy of rat liver sections showing distribution of endocytosed Texas red-dextran (A, C, E, G) and G_β (B, D, F, H) in the same image. A, B: Control liver exposed to dextran for 2 minutes. C, D: CTX-treated liver exposed to dextran for 2 minutes. E, F: Control liver exposed to dextran for 20 minutes G, H: CTX-treated liver exposed to dextran for 20 minutes. Arrows point to punctate G_β staining in the pericanalicular area (B, F, H) and region of punctate autofluorescence (A) or corresponding endocytosed Texas red-dextran (E, G), arrowheads point to punctate G_β staining in the perinuclear area in CTX-treated livers (D, H) and region of punctate autofluorescence (C) or corresponding endocytosed Texas red-dextran (G) and asterisks mark representative sinusoidal spaces. Images are representative of 10 (A, B), 30 (C, D), 36 (E, F) and 39 (G, H) images examined from 1, 1, 5 and 4 livers, respectively.

exocytosis. In CTX-treated livers, $G_{s\alpha}$ antibody also stained punctate perinuclear structures that corresponded to mis-trafficked Texas red-dextran (arrows, Figures 6E,6F).

Antibody to $G_{i\alpha1,2}$ (Figures 7B,7D) stained predominantly cytoplasm and nuclei. Because of the cytoplasmic staining, concurrence between Texas red-dextran and $G_{i\alpha1,2}$ could not be identified (Figures 7A/B,7C/D). Antibody to $G_{i\alpha3}$ (Figures 7F,7H) also produced granular cytoplasmic staining, however linear/punctate staining at both BLM and CM (arrows) could be appreciated after 2 minutes (Figure 7F) or 20 minutes (Figure 7H) of dextran endocytosis. Overlap of dextran fluorescence and antibody staining of $G_{i\alpha3}$ could be identified, especially near the CM (arrows, Figures 7G,7H).

Antibody to G_β stained cytoplasm and, in control livers nuclei, but prominently labelled the BLM as well as punctate structures in the perisinusoidal and pericanalicular (arrows) regions of liver from control (Figures 8B,8F) or CTX-treated (Figures 8D,8H) livers. Punctate staining was also identified in perinuclear clusters (arrowheads, Figures 8D,8H) in CTX-treated livers. Many areas of overlap between Texas red-dextran fluorescence and G_β staining were identified near the BLM after 2 minutes of dextran endocytosis (Figures 8A/B,8C/D), near the BLM and CM after 20 minutes of dextran endocytosis (Figures 8E/F,8G/H) and, in CTX-treated livers, near the nuclei (Figures 8G/H).

Confocal microscopy was employed also to try to localize rab 5 as this GTP-binding protein was distributed on gradients in a pattern similar to heterotrimeric G protein subunits and FITC-dextran (Figure 4). In liver rab 5 would be expected to associate with early endosomes near BLM and CM, rather than with more mature CURL/MVB/lysosomes. Faint specific staining was identified in a linear pattern along BLM and CM, diffusely throughout the cytoplasm and as denser diffuse staining in regions where dextran-containing vesicles were visualized, adjacent to BLM and CM and, in CTX-treated livers, in perinuclear regions (data not shown). However, the low level of rab 5 staining precluded any definite conclusions regarding colocalization of rab 5 and dextran-loaded endosomes.

Discussion

Endosomes internalize integral plasma membrane and membrane-associated proteins, which subsequently can be recycled back to the plasma membranes, transported to other membranes and/or delivered to lysosomes or proteasomes for degradation [30]. For many proteins endocytosis is simply a mechanism for transportation from one location to another, however internalized receptors and other proteins may function and be regulated in unique ways [2,5,7,9,36] and thus endosomes are not simply

cargo vessels. For example, internalized β_2 adrenergic receptor and β-arrestins contribute to formation of signalling complexes and may initiate unique signalling pathways [2,8]. Signal transduction from circulating hormones is a critical function of hepatocyte plasma membranes. Although intracellular signalling from insulin receptors has been well characterized in liver [2,5-8,36], little is known regarding the role of endocytosis in signalling from GPCRs involved in cAMP-mediated signal transduction [2,8,11], especially as regards the physical location of heterotrimeric G protein subunits that couple to GPCRs in liver.

Further, previous studies suggested that signalling through Gs and Gi proteins may, in turn, alter endocytosis and endosome trafficking [11,16,17,37]. Therefore a systematic study was undertaken to determine whether heterotrimeric G protein subunits were associated with hepatocyte endosomes as the first step in assessing whether internalized GPCR, like insulin and EGF receptors, can generate signals from endosomes.

Three different approaches were used in the present study. First, Western blotting was performed with purified endocytic vesicles and plasma membranes. Although the principal goal was to identify heterotrimeric G protein subunits on intracellular endocytic vesicles, a second goal was to compare/contrast the rank order of G proteins with other marker proteins as evidence for internalization and recycling and against contamination of vesicles by plasma membranes.

A plasma membrane preparation was selected that is considered free of intracellular organelles, although exhibiting 8% contamination of BLM with CM [38]. However, CM proteins may traffic from Golgi-to-BLM-to-CM [39] and therefore be found on BLM as well. As few methods are available to purify rat liver endosomes, clathrin-coated vesicles, the earliest stage of receptor-mediated endocytosis, also exist in Golgi, and heterotrimeric G proteins may be internalized in non-coated vesicles [1], a method was chosen that allows simultaneous preparation of three different types of endocytic vesicles, representing different steps in receptor-mediated endocytosis and destinations for probes of fluid-phase endocytosis [18-20]. These vesicles have been used to study liver receptor-mediated and fluid-phase endocytosis, endosome ion transport and association of proteins with endosomes [18-24,31]. During receptor-mediated endocytosis recycling receptors are found in these vesicles in the order RRC>CURL>MVB [17,19,23,24,30]. Purified secondary lysosomes [25] were studied also as internalized proteins destined for degradation are transferred from early endosomes to CURL, to MVB and on to lysosomes. Such proteins are enriched in the order MVB>CURL>RRC [18,19,21,23,24]. Heterot-

rimeric G protein subunits may be degraded primarily via ubiquination and proteasomes [40], thus little likely enters lysosomes.

By Western blotting three Gα and one Gβ subunit were found on CM and BLM, qualitatively similar to the results of others using different membrane preparative methods [3,4]. These G protein subunits were found in the order CM $\geq$BLM>>>RRC>CURL$\geq$MVB$\geq$lysosomes (Figure 1), an order expected for proteins endocytosed and then recycled back to the plasma membrane and similar to the order identified for Trf-R (Figure 2) [23,24,30]. Others identified a similar order for other signalling molecules including EGF receptors, Ras, Raf-1, MAPK kinase, MAPK and phospho-MAPK [6,9,19,24]. The heterotrimeric G protein subunits likely were attached to the cytoplasmic surface of endosomes, a position that allows signal transduction. However MVB internalize their own membranes as topographically inverted internal vesicles [41], thus some of these G proteins may be delivered to lysosomes as internalized cargo.

These results agree with those of others who identified G$_{s\alpha}$ and generic G$_{i\alpha}$ on RRC, CURL and MVB in the same order (Figure 1) [24,31]. Further we also identified the G$_s$ effector AC on CM, BLM and endocytic vesicles (Figure 5). AC activity, but not protein content, was previously demonstrated on liver BLM and CM [3]. Collectively these findings confirm and extend the observations of others and support the hypothesis that heterotrimeric G proteins may participate in intracellular signal transduction.

Western blot methods critically depend on the purity of the samples. Given the large amount of G$_{s\alpha}$, G$_{i\alpha1,2}$, G$_{i\alpha3}$ and G$_\beta$ on CM and BLM (Figure 1), contamination of endosomes with up to 5–30% CM or BLM might explain the results. This high a contamination seems unlikely, but merits serious consideration. Therefore the distribution, in vesicles, of other plasma membrane proteins was examined. If contamination was the explanation, all should have exhibited the same pattern (rank order). G$_{s\alpha}$, G$_{i\alpha1,2}$, G$_{i\alpha3}$ and G$_\beta$ were found in the same order identified for recycling receptors and the α_1 subunit of Na, K-ATPase (Figure 2). By contrast, MDR-1 and MRP-2, which likely traffic from Golgi-to-BLM-to-CM and are subsequently endocytosed from CM and degraded in lysosomes [32-34,39] were detected in the order MVB > CURL~RRC, similar to the order of endocytosed proteins degraded in lysosomes [18,19,21,23,24].

We also examined distribution of rab 5 and rab 4, markers of early and recycling endosomes [29,30], respectively, that are also associated with plasma membranes. RRC as a combination of early, recycling and transcytotic vesicles [22] are expected to exhibit rab 4 and rab 5 while receptor-

containing appendages of CURL [18] might exhibit rab 4. Others found both rabs in the order RRC$\geq$CURL>MVB [22-24]. However, using the same antibodies we were unable to identify rabs in our endosomes (Figure 3), possibly as our x-ray films may not have been exposed as long due to large amounts of rabs on plasma membrane samples. Conversely, the absence of detectable rab 5 and rab 4 in our endosomes suggests that contamination of endosomes by CM or BLM must be small.

Quantitative study of the distribution of Na, K-ATPase α_1 and β_1 subunits also suggested little contamination of endocytic vesicles by plasma membranes. As previously reported by others for different membrane preparations [26], both subunits were detected in CM and BLM with β_1 in larger amounts in BLM. In intracellular vesicles α_1 was detected in the order RRC>CURL>MVB>lysosomes, the same found for G$_{s\alpha}$, G$_{i\alpha1,2}$, and G$_\beta$ (Figure 1) and recycling receptors, which suggests α_1 is internalized and recycled. Others identified α_1 only in RRC [22], suggesting differences in techniques or antibody lot. Although β_1 could not be identified in our vesicles (Figure 2), β_1 is found in rat liver early endosomes [42]. Since the antibody employed was capable of demonstrating β_1 in even small amounts of BLM (Figure 2), the lack of β_1 in RRC/CURL/MVB/lysosomes is likely due to rapid loss of β_1 after endocytosis by ubiquination and proteasome degradation [28], resulting in high α/β ratio [27].

A second method for demonstrating colocalization of proteins and intracellular vesicles is the pattern of distribution on density gradients. We used PNS to minimize bias from selective loss of any cellular organelles and to complement the experiments performed using highly purified plasma membranes and endocytic vesicles. G$_{s\alpha}$, G$_{i\alpha3}$ and G$_\beta$ were readily detectable throughout most of the gradient, paralleling detection of endocytosed FITC-dextran, even in regions of the gradient where markers of plasma membranes and Golgi vesicles were minimally detected (Figure 4). G$_{i\alpha1,2}$, however, was identified principally in regions where the bulk of endosomes and the trans-Golgi network (identified by TGN-38) were found, consistent with reports in other cell types [14,15]. Clean separation of plasma membranes from low density intracellular organelles on such gradients is not possible [15], therefore the results shown here do not constitute conclusive proof. However these findings are consistent with presence of at least some heterotrimeric G protein subunits on endocytic vesicles.

The third approach was direct visualization of G$_{s\alpha}$, G$_{i\alpha1,2}$, G$_{i\alpha3}$ and G$_\beta$ by confocal microscopy of liver in which endosomes were labelled by the endocytosed fluid phase marker Texas red-dextran [17]. Major advantages of confocal microscopy include verification that these proteins

are in hepatocytes and the ability to identify co-localization with endocytosed probes. We previously showed that fluorescent dextrans endocytosed from blood at the BLM first appear in punctate vesicles just under the BLM and then rapidly traffic, presumably on microtubules, to the pericanalicular region where endosomes, lysosomes and elements of the Golgi Apparatus are found [17]. Vesicles endocytosed from the CM [34] are not labelled with Texas red-dextran. In CTX-treated livers, mistrafficked early and late endosomes form perinuclear clusters, spatially separated from BLM and CM [17].

$G_{s\alpha}$, $G_{i\alpha3}$ and G_β were identified on CM and BLM, consistent with limited previous studies of mouse liver [43] and with Western blots (Figure 1) [3,26]. In addition punctate staining was identified adjacent to and under CM and BLM, a pattern interpreted as indicating protein in, or attached to, vesicles, including endosomes. This punctate staining was visible near CM after two minutes of dextran endocytosis when no dextran-loaded endosomes were found there, ruling out bleed-through from the Texas red signal (Figures 6B,7F,8B). Punctate staining also was found in perinuclear regions in CTX-treated livers (Figures 6F,8H), where staining of plasma membranes could not create artifacts. These findings provide strong support for our hypothesis that heterotrimeric G proteins are indeed located on endocytic vesicles.

$G_{i\alpha3}$ was observed also faintly distributed over the cytoplasm, although not in a pattern specific to any known organelle. Others have identified $G_{i\alpha3}$ by immunofluorescence on plasma membranes, nuclei, Golgi Apparatus and in subapical compartments in a variety of cell types [14,15,43,44].

We were unable to localize $G_{i\alpha1,2}$ to membranes or endocytic vesicles due to the intense nuclear and diffuse cytoplasmic staining. This finding differs from the ready detection of $G_{i\alpha1,2}$ on membranes and endosomes by Western blotting (Figure 1), but may reflect inadequacies of the antibody to detect the native protein in fixed tissue or the concurrent localization of this G protein to other organelles [14,15]. Indeed others have identified $G_{i\alpha1,2}$ by immunofluorescence in many locations including cytosol, on intracellular organelles, nuclei, actin filaments and/or on plasma membranes [14,15,43,44]. Thus no definitive conclusions can be drawn from the confocal microscopy studies regarding membrane localization of $G_{i\alpha1,2}$.

Conclusions
In conclusion, our studies provide strong support from three different methods that some heterotrimeric G protein subunits are present on endocytic vesicles, possibly with other signalling machinery such as AC (Figure 5) and

PKA [10]. Thus, in hepatocytes, GPCR and signal transduction machinery may be internalized and signal from sites spatially separated from plasma membranes. Definitive proof of this hypothesis will require additional research to look for evidence of signalling activity in liver endosomes.

Methods
Materials
Chemicals were obtained from Sigma (St. Louis, MO) and Bio-Rad Laboratories (Hercules, CA). 10,000 Da Texas red-dextran, 70,000 Da FITC-dextran, FITC-WGA and antifluorescein Alexa 488 amplification kits were from Molecular Probes (Eugene, OR), CTX from List Biological Laboratories (Campbell, CA), nitrocellulose membranes and hyperfilm from Amersham Life Science (Little Chalfont, England) and SuperSignal chemiluminescence reagents from Pierce (Rockford, IL).

Antibodies
Rabbit antibodies to $G_{s\alpha}$, $G_{i\alpha1,2}$, $G_{i\alpha3}$ and G_β from DuPont NEN Research (Boston, MA) were used at 1:1,000 (blotting) and 1:50 – 1:100 (G_β immunofluorescence). Rabbit antibodies to $G_{s\alpha}$ (Ab951), $G_{i\alpha1,2}$ (Ab982) and $G_{i\alpha3, O}$ (Ab976) from Dr. Thomas Gettys (Medical University of South Carolina) [45-47] were used at 1:100 for immunofluorescence. The latter two likely identify $G_{i\alpha2}$ and $G_{i\alpha3}$ in liver. Standards for $G_{s\alpha}$, $G_{i\alpha2}$ and $G_{i\alpha3}$ were from Calbiochem (LaJolla, CA). Polyclonal antibodies to rab 4, rab 5a, AC V/VI [48-50] and LAMP1 from Santa Cruz Biotechnology (Santa Cruz, CA) were used at 1:100, 1:100, 1:50 and 1:200, respectively. Rabbit antibody MDR-Ab1 from Oncogene Research Products (Cambridge, MA) detects mdr1a and mdr2 in rodent liver [51] and was used at 1:20. Rabbit antibody to MRP-2 from Dr. Dietrich Keppler (University of Heidelberg) was used at 1:50,000. Monoclonal antibodies to Trf-R (Zymed Laboratories, South San Francisco, CA), EEA1 (Transduction Laboratories, Lexington, KY) and TGN-38 (Affinity BioReagents, Golden, CO) were used at 1:1000, 1:50 and 1:500, respectively. Standards and monoclonal antibodies to α_1 and β_1 subunits of Na, K-ATPase from Upstate Biotechnology (Lake Placid, NY) were used at 1:200 and 1:500, respectively. Polyclonal antibody to rab 5 (Stressgen Biotechnologies, Victoria, B.C., Canada) was used at 1:100 for immunofluorescence. Secondary antibodies conjugated to horseradish peroxidase (HRP), FITC or Cy5 and preimmune sera were from Zymed and Jackson Immunoresearch Laboratories (West Grove, PA).

Animals
Male Sprague-Dawley rats (250–350 g) were from Harlan Sprague-Dawley (Indianapolis, IN) and received humane care according to guidelines from the National Academy of Sciences. Studies were approved by the local IACUCs.

Animals were used to prepare homogenates, PNS, endosomes (CURL, RRC and MVB) and lysosomes [17,18,20,25]. BLM and CM [38] were a gift from Dr. Richard Moseley (University of Michigan). As indicated in text and figure legends, some rats were injected 16 hours before use with 120 μg/kg CTX to alter endosome trafficking. Some rats were injected intravenously with 25 mg Texas-red-dextran or 75 mg FITC-dextran to label endosomes [17]. For immunofluorescence livers were perfusion-fixed, cryoprotected and frozen 2 and 20 minutes after dextran administration [17].

Percoll gradient fractionation
Rat liver PNS was fractionated on Percoll gradients [17] and plasma membranes were identified by FITC-WGA binding and APDE I activity [17].

Western blots
Samples were separated on polyacrylamide gels and proteins transferred electrophoretically to nitrocellulose [17]. For most studies equal amounts of protein were loaded into each well and one well contained CM. Standards for $G_{s\alpha}$, $G_{i\alpha2}$, $G_{i\alpha3}$ and Na, K-ATPase subunits were run as positive controls. Blots were blocked and antibody-bound for 2–16 hours with primary antibody and 30–60 minutes with HRP-conjugated secondary antibodies in Tris buffered saline with Tween and 5% milk [17]. For AC high salt buffers were substituted [48]. Bands detected by chemiluminescence using Super Signal were recorded on x-ray film. Conditions were optimized for each protein-antibody pair. X-ray film was scanned and integrated optical density of bands determined using calibrated NIH Image software. The linear range for optical density with respect to protein concentration and exposure time was determined and used for all analyses. Optical densities of bands from BLM or vesicles were divided by the optical density of bands from CM on the same blot to "normalize" values and allow comparison of values between different blots. CM samples were chosen as they exhibited the highest amount of G protein subunits and are considered clean [38].

Immunofluorescence
Cryostat sections of fixed and frozen rat livers were cut, treated and antibody-bound as described [17]. For $G_{s\alpha}$, $G_{i\alpha1-2}$ and $G_{i\alpha3}$, detection was enhanced by an anti-fluorescein Alexa 488 amplification kit. Images optically sectioned at 1 μm were obtained using a Bio-Rad MRC 600 confocal microscope (Hercules, CA) and processed using Adobe Photoshop (Adobe Systems, San Jose, CA) [17]. Control sections incubated with pre-immune serum or in the absence of primary or secondary antibodies with or without Alexa 488 amplification were imaged with FITC, Cy5 and Texas red wavelengths to confirm both antibody specificity and that results were not due to autofluorescence or bleed-through of signal. Images were displayed in black and white as the intense Texas red fluorescence overwhelmed fluorescence from G protein antibodies when images were superimposed.

Calculations and Statistics
Mean ± SEM were calculated for optical densities of bands on Western blots expressed as a ratio of values from CM on the same blot. Student's t test was used to compare these values to a value of "0", the value assigned when no band could be detected. $P < 0.05$ was taken to indicate statistical significance.

Abbreviations
adenylate cyclase AC

alkaline phosphodiesterase I APDE I

basolateral membrane BLM

canalicular membrane CM

cholera toxin CTX

compartment for uncoupling of receptor and ligand CURL

early endosome antigen 1 EEA1

epidermal growth factor EGF

fluorescein isothiocyanate FITC-dextran

G protein coupled-receptor GPCR

horseradish peroxidase HRP

lysosome associated membrane protein 1 LAMP1

MDR-related protein 2 MRP-2

mitogen-activated protein kinase MAPK

multi-drug resistance protein MDR

multivesicular bodies MVB

phosphate buffered saline PBS

post-nuclear supernatant PNS

protein kinase A PKA

recycling receptor compartment RRC

transferrin receptor Trf-R

trans-Golgi network protein 38 TGN-38

wheat germ agglutinin WGA

Authors' contributions

RWVD conceived and designed the study, performed part of the animal and Percoll gradient studies, analyzed data and wrote the manuscript. Research technicians MRL, DWB, LLF, AK and XW participated in animal and Percoll gradient studies and performed Western blot studies and MRL performed the confocal microscopy studies.

Acknowledgements

References

1. Pike LJ: **Lipid rafts: bringing order to chaos.** *J Lipid Res* 2003, **44**:655-667.
2. Ferguson SSG: **Evolving concepts in G protein-coupled receptor endocytosis: the role in receptor desensitization and signaling.** *Pharmacological Reviews* 2001, **53**:1-24.
3. Dixon BS, Sutherland E, Alexander A, Nibel D, Simon FR: **Distribution of adenylate cyclase and GTP-binding proteins in hepatic plasma membranes.** *Am J Physiol* 1993, **265**:G686-G698.
4. Ali N, Milligan G, Evans WH: **Distribution of G-proteins in rat liver plasma-membrane domains and endocytic pathways.** *Biochem J* 1989, **261**:905-912.
5. Bevan AP, Drake PG, Bergeron JJM, Posner BI: **Intracellular signal transduction: The role of endosomes.** *Trends in Endocrin Metab* 1996, **7**:13-21.
6. Faure R, Gaulin JF, Bourgoin S, Fortier S: **Compartmentalization of the mitogen-activated protein kinase (MAPK) in hepatic endosomes: association with the internalized epidermal growth factor (EGF) receptor.** *Mol Cell Biol Res Commun* 1999, **1**:132-139.
7. Balbis A, Baquiran G, Bergeron JJM, Posner BI: **Compartmentalization and insulin-induced translocations of insulin receptor substrates, phosphatidylinositol 3-kinase, and protein kinase B in rat liver.** *Endocrinology* 2000, **141**:4041-4049.
8. Daaka Y, Luttrell LM, Ahn S, Della Rocca GJ, Ferguson SSG, Caron MG, Lefkowitz RJ: **Essential role of G protein-coupled receptor endocytosis in the activation of mitogen-activated protein kinase.** *J Biol Chem* 1998, **273**:685-688.
9. Pol A, Calvo M, Enrich C: **Isolated endosomes from quiescent rat liver contain the signal transduction machinery: differential distribution of activated Raf-1 and Mek in the endocytic compartment.** *FEBS Lett* 1998, **441**:34-38.
10. Van Dyke RW, Root KV, Hsi RA: **cAMP and protein kinase A stimulate acidification of rat liver endosomes in the absence of chloride.** *Biochem Biophys Res Comm* 1996, **222**:312-316.
11. Zheng B, Ma Y-C, Ostrom RS, Lavoie C, Gill GN, Insel PA, Huang X-Y, Farquhar MG: **RGS-PX1, a GAP for G$_{\alpha s}$ and sorting nexin in vesicular trafficking.** *Science* 2001, **294**:1939-1942.
12. Codina J, Gurich R, DuBose TD Jr: **Peptides derived from the human transferrin receptor stimulate endosomal acidification via a G$_i$-type protein.** *Kidney International* 1999, **55**:2376-2382.
13. Griffiths G, Hollinshead R, Hemmings BA, Nigg EA: **Ultrastructural localization of the regulatory (RII) subunit of cyclic AMP-dependent protein kinase to subcellular compartments active in endocytosis and recycling of membrane receptors.** *J Cell Sci* 1990, **96**:691-703.
14. Stow JL, de Almeida JB: **Distribution and role of heterotrimeric G proteins in the secretory pathway of polarized epithelial cells.** *J Cell Sci Suppl* 1993, **17**:33-39.
15. Denker SP, McCaffery JM, Palade GE, Insel PA, Farquhar MG: **Differential distribution of α subunits and $\beta\gamma$ subunits of heterotrimeric G proteins on Golgi membranes of the exocrine pancreas.** *J Cell Biol* 1996, **133**:1027-1040.
16. Helms JB: **Role of heterotrimeric GTP binding proteins in vesicular protein transport: indications for both classical and alternative G protein cycles.** *FEBS Lett* 1995, **369**:84-88.
17. Van Dyke RW: **Effect of cholera toxin and cyclic adenosine monophosphate on fluid phase endocytosis, distribution and trafficking of endosomes in rat liver.** *Hepatology* 2000, **32**:1357-1369.
18. Belcher JD, Hamilton RL, Brady SE, Hornick CA, Jaeckle S, Schneider WJ, Havel RJ: **Isolation and characterization of three endosomal fractions from the liver of estradiol-treated rats.** *Proc Natl Acad Sci USA* 1987, **84**:6785-6789.
19. Jackle S, Runquist EA, Brady SM, Havel RJ: **Trafficking of the epidermal growth factor receptor and transferrin in three hepatocytic endosomal fractions.** *J Biol Chem* 1991, **266**:1396-1402.
20. Van Dyke RW, Belcher JD: **Acidification of three types of liver endocytic vesicles: similarities and differences.** *Amer J Physiol* 1994, **266**:C81-C94.
21. Enrich C, Jäckle S, Havel RJ: **The polymeric immunoglobulin receptor is the major calmodulin-binding protein in an endosome fraction from rat liver enriched in recycling receptors.** *Hepatology* 1996, **24**:226-232.
22. Enrich C, Pol A, Calvo M, Pons M, Jäckle S: **Dissection of the multifunctional "receptor-recycling" endocytic compartment of hepatocytes.** *Hepatology* 1999, **30**:1115-1120.
23. Verges M, Havel RJ, Mostov KE: **A tubular endosomal fraction from rat liver: biochemical evidence of receptor sorting by default.** *Proc Natl Acad Sci USA* 1999, **96**:10146-10151.
24. Calvo M, Enrich C: **Biochemical analysis of a caveolae-enriched plasma membrane fraction from rat liver.** *Electrophoresis* 2000, **21**:3386-3395.
25. Van Dyke RW: **Acidification of rat liver lysosomes: quantitation and comparison with endosomes.** *Am J Physiol* 1993, **265**:C901-C917.
26. Simon FR, Fortune J, Alexander A, Iwahashi , Dahl R, Sutherland E: **Increased hepatic Na, K-ATPase activity during hepatic regeneration is associated with induction of the β_1-subunit and expression on the bile canalicular domain.** *J Biol Chem* 1996, **271**:24967-24975.
27. McDonough AA, Geering K, Farley RA: **The sodium pump needs its β subunit.** *FASEB J* 1990, **4**:1598-1605.
28. Yoshimura SH, Hizume K, Takeyasu K: **Differential degradation of the Na/K-ATPase subunits in the plasma membrane [abstract].** *Mol Biol Cell* 2001, **12**:69a.
29. Deneka M, van der Sluijs P: **'Rab'ing up endosomal membrane transport.** *Nature Cell Biol* 2002, **4**:E33-E35.
30. Mukherjee S, Ghosh RN, Maxfield FR: **Endocytosis.** *Physiol Rev* 1997, **77**:759-803.
31. Pol A, Enrich C: **Membrane transport in rat liver endocytic pathways: preparation, biochemical properties and functional roles of hepatic endosomes.** *Electrophoresis* 1997, **18**:2548-2557.
32. Hayes JH, Soroka CJ, Rios-Velez L, Boyer JL: **Hepatic sequestration and modulation of the canalicular transport of the organic cation, daunorubicin, in the rat.** *Hepatology* 1999, **29**:483-493.
33. Roelofsen H, Soroka CJ, Keppler D, Boyer JL: **Cyclic AMP stimulates sorting of the canalicular organic anion transporter**

(Mrp2/cMoat) to the apical domain in hepatocyte couplets. *J Cell Sci* 1998, **111:**1137-1145.

34. Rahner C, Stieger B, Landmann L: **Apical endocytosis in rat hepatocytes in situ involves clathrin, traverses a subapical compartment, and leads to lysosomes.** *Gastroenterology* 2000, **119:**1692-1707.

35. Simonds WF: **G protein regulation of adenylate cyclase.** *TiPS* 1999, **20:**66-73.

36. Contreres J-O, Faure G, Baquiran G, Bergeron JJ, Posner BI: **ATP-dependent desensitization of insulin binding and tyrosine kinase activity of the insulin receptor kinase: the role of endosomal acidification.** *J Biol Chem* 1998, **273:**22007-22013.

37. Lin HC, Duncan JA, Kozasa T, Gilman AG: **Sequestration of the G protein βγ subunit complex inhibits receptor-mediated endocytosis.** *Proc Natl Acad Sci USA* 1998, **95:**5057-5060.

38. Meier PJ, Sztul ES, Reuben A, Boyer JL: **Structural and functional polarity of canalicular and basolateral plasma membrane vesicles isolated in high yield from rat liver.** *J Cell Biol* 1984, **98:**991-1000.

39. Tuma PL, Nyasae LK, Hubbard AL: **Nonpolarized cells selectively sort apical proteins from cell surface to a novel compartment, but lack apical retention mechanisms.** *Mol Biol Cell* 2002, **13:**3400-3415.

40. Botion LM, Brasier AR, Tian B, Udupi V, Green A: **Inhibition of proteasome activity blocks the ability of TNF alpha to downregulate G(i) proteins and stimulate lipolysis.** *Endocrinology* 2001, **142:**5069-5075.

41. Katzmann DJ, Odorizzi G, Emr SD: **Receptor downregulation and multivesicular-body sorting.** *Nature Reviews Mol Cell Biol* 2002, **3:**893-905.

42. Casciola-Rosen LA, Hubbard AL: **Lumenal labeling of rat hepatocyte early endosomes.** *J Biol Chem* 1992, **267:**8213-8221.

43. Cadrin M, McFarlane-Anderson N, Harper ME, Gaffield J, Begin-Heick N: **Comparison of the subcellular distribution of G-proteins in hepatocytes in situ and in primary cultures.** *J Cell Biochem* 1996, **62:**334-341.

44. Wilson BS, Komuro M, Farquhar MG: **Cellular variations in heterotrimeric G protein localization and expression in rat pituitary.** *Endocrinology* 1994, **134:**233-244.

45. Gettys TS, Ramkumar V, Surwit RS, Taylor IL: **Tissue-specific alterations in G protein expression in genetic versus diet-induced models of non-insulin-dependent diabetes mellitus in the mouse.** *Metabolism* 1995, **44:**771-778.

46. Palmer TM, Gettys TW, Stiles GL: **Differential interaction with and regulation of multiple G-proteins by the rat A^3 adenosine receptor.** *J Bio Chem* 1995, **270:**16895-16902.

47. Bouscarel B, Matsuzaki Y, Le M, Gettys TW, Fromm H: **Changes in G protein expression account for impaired modulation of hepatic cAMP formation after BDL.** *Am J Physiol* 1998, **274:**G1151-G1159.

48. Liu CY, Jamaleddin AJ, Zhang H, Christofi FL: **F1CRhR/cyclic AMP signaling in myenteric ganglia and calbindin-D28 intrinsic primary afferent neurons involves adenylyl cyclases I, III and IV.** *Brain Res* 1999, **826:**253-269.

49. Ostrom RS, Gregorian C, Drenan RM, Xiang Y, Regan JW, Insel PA: **Receptor number and caveolar co-localization determine receptor coupling efficiency to adenylyl cyclase.** *J Bio Chem* 2001, **276:**42063-42069.

50. Rossler P, Kroner C, Krieger J, Lobel D, Breer H, Boekhoff I: **Cyclic adenosine monophosphate signaling in the rat vomeronasal organ: role of an adenylyl cyclase type VI.** *Chem Senses* 2000, **25:**313-322.

51. Fontana RJ, Lown KS, Paine MF, Fortlage L, Santella RM, Felton JS, Knize MG, Greenberg A, Watkins PB: **Effects of a chargrilled meat diet on expression of CYP3A, CYP1A, and P-glycoprotein levels in healthy volunteers.** *Gastroenterology* 1999, **117:**89-98.